A Nonlinear Model Combining Pulmonary Mechanics and Gas Concentration Dynamics

KENNETH R. LUTCHEN, STUDENT MEMBER, IEEE, FRANK P. PRIMIANO, JR., MEMBER, IEEE, AND GERALD M. SAIDEL

Abstract—To elucidate the various mechanisms by which pulmonary mechanics affect the distribution of gas species throughout the lungs, a multicompartment model relating pressure differences, flows, volumes, and gas species concentrations has been developed. The alveolar regions of the model are nonlinearly elastic and the pressure-flow relation of their associated small airways is volume dependent. Various combinations of parameter values were chosen, including cases in which the model was mechanically uniform (normal) and nonuniform (obstructive). Computer solutions of model equations were obtained for both piecewise-exponential and sinusoidal transpulmonary pressure inputs. Clinical measures of mechanical uniformity and gas concentration homogeneity were evaluated along with unobservable indexes. Results indicate how the distribution of mechanical variables affects the distribution of gas species concentration within the lungs. For the nonuniform (obstructive) model, the gas is distributed more inhomogeneously at higher frequencies and lower lung volumes. The distribution of initial dead space gas to the compartments as well as pendelluft tend to decrease this inhomogeneity. Dynamic compliance for the nonuniform model was frequency dependent at each of the three volume operating points investigated, whereas the semilog nitrogen washout curve was essentially linear for some frequencies and volumes while nonlinear for others. Consequently, inferences about distributions of mechanical parameters and intrapulmonary gas may require that clinical measurements be obtained together at several frequencies and volume operating points.

List of Key Symbols

C_i—tracer concentration in alveolar compartment i
$\dot{C}_i$—rate of change of C_i
C_m—tracer concentration at mixing node m
$C(0)$—initial tracer concentration throughout the lung
C_{in}—tracer concentration of inspired gas
C_{1m}—tracer concentration entering the mixing node from the dead space
C_{ao}—tracer concentration at the airway opening
$GDI(i)$—generalized dilution index of alveolar compartment i
k—breath number
P_{tp}—transpulmonary pressure difference
Q_{ao}—flow rate at airway opening
Q_i—flow rate in compartment i; $i = 1, 2, 3$
$SDI(i)$—simple dilution index of alveolar compartment i
V_i—volume of compartment i
V_D—volume of dead space
V_L—total lung volume
$\dot{V}_i$—rate of change of V_i
$\dot{V}_L$—rate of change of V_L
V_{Ti}—tidal volume of compartment i
V_T—tidal volume of pulmonary system (integrated flow at airway opening over an inspiration)
v_L—change in lung volume from the beginning of an inspiration or expiration
$V_i(E)$—end-expiratory volume of alveolar compartment i
$V_i(t_D)$—volume of alveolar compartment i at time at which V_D is cleared during inspiration
V_P/V_T—pendelluft volume fraction
X_i—normalized tracer concentration; $i = 1, 2, 3, 1m, m, in$
$\overline{\Delta X}$—mean value of the normalized, end-tidal, alveolar concentration difference over a multibreath washout
Y—normalized tracer concentration of the airway opening

Greek Symbols

η_k—dilution number
θ_j—time delay for clearance of any incremental volume of gas entering the dead space at time t_j during expiration or inspiration
λ_i—fraction of the end-expiratory gas volume in V_D which is distributed to $V_i (i = 2, 3)$ during the subsequent inspiration
μ_1/μ_0—mean dilution number (ratio of first to zeroth moment)

Manuscript received August 5, 1981; revised February 24, 1982. This work was supported in part by the Medical Research Service of the Veterans Administration under Grants HL-07414 and AM-08305. The work of K. R. Lutchen was also supported in part by a summer Fellowship from the Northern Ohio Lung Association and by the National Institutes of Health under Predoctoral Traineeship Grant GM-07535.

K. R. Lutchen is with the Department of Biomedical Engineering, Case Western Reserve University, Cleveland, OH 44106.
F. P. Primiano, Jr. is with the Departments of Biomedical Engineering and Pediatrics, Case Western Reserve University, Cleveland, OH 44106, and the Rainbow Babies and Children's Hospital, Cleveland, OH 44106.
G. M. Saidel is with the Department of Biomedical Engineering, Case Western Reserve University, Cleveland, OH 44106, and the Veterans Administration Medical Center, Cleveland, OH 44106.

Introduction

FOR several decades, investigators have hypothesized numerous cause and effect relations between pulmonary mechanical function and the distribution of gas concentrations throughout the lungs. In pulmonary mechanics, major emphasis has been on modeling the lungs as a linear system acting about fixed volume-pressure operating points [13]. The lungs are often depicted as a parallel combination of compartments each with a distinct resistance and compliance. Analyses demonstrate that unequal mechanical time constants (products of resistance and compliance) of the representative alveolar compartments cause asynchronous flows among the compartments and, hence, nonuniform distribution of inspired air. However, knowledge of the pattern of compartmental tidal volumes, which is all that these models provide, is insuf-

0018-9294/82/0900-0629$00.75 © 1982 IEEE

ficient to determine the distribution of gas species concentrations throughout the lungs. In fact, to fully understand the relation between pulmonary mechanics and gas concentration dynamics, one must investigate the effects of compartmental end-expiratory volumes, the distribution of dead space gas to the compartments, and intercompartmental gas mixing, as well as the distribution of tidal volumes.

To adequately demonstrate how each of these aspects of pulmonary behavior (particularly those associated with changes in end-expiratory volume) influence gas species concentration distribution, the nonlinear relations among pulmonary mechanical variables must be included. Nonlinear models have previously been used to relate mechanics and gas concentration distribution under various circumstances. For example, Pedley *et al.* [14] developed a two-compartment model that incorporated nonlinear pressure–volume and pressure–flow relationships. They were able to simulate a wide range of single breath, constant-flow, vital capacity washins of a tracer gas. However, nonlinear models which can describe mechanical and gas concentration dynamics during cyclic, tidal volume breathing and which include asynchronous compartmental flows have not been reported. The purpose of this paper is to present a nonlinear mathematical model which includes sufficient detail to describe the functional relations between pulmonary mechanics and gas concentration dynamics during breathing at various frequencies and volume operating points.

Statement of the Problem

We define a multicompartment pulmonary system to be mechanically *uniform* if, for *all physiological* breathing patterns and volume operating points, it acts as a single mechanical compartment. A single-compartment mechanical system is one with only a single degree of freedom. The movement of such a system can be described by one displacement variable, namely, a compartmental volume change. Hence, for a multicompartment lung to act as a single compartment system, the flow into all lung compartments must be synchronous and in the same direction under all physiological conditions. If a system is linear, the only requirement for uniformity is that the mechanical time constants of all compartments be equal. In this case the ratios of compartmental flows and, consequently, the *ratios* of their tidal volumes are constant throughout the breathing cycle at all breathing rates. For a nonlinear, multicompartment system, however, a sufficient condition that the flows will be synchronous and in the same direction for all physiological breathing patterns and operating points is that the compartments have identical mechanical relations. Whether this is a necessary condition is not obvious.

The distribution of gas species concentrations throughout the lung can be analyzed by multicompartment mass-transport models. These models usually comprise several perfectly mixed alveolar compartments connected to a common dead space which acts as a pure time delay. We define the distribution of a tracer gas among all alveolar compartments as *homogeneous* when the gas phase dynamics of a tracer gas (i.e., insoluble, inert species) are such that there exist equal concentrations of the tracer gas in all alveolar compartments at all times. That is, the gas phase dynamics can be described as though they occur in a system comprising a *single*, perfectly mixed alveolar compartment with a dead space. Thus, for all physiological breathing patterns and operating points, a multibreath washout (or washin) of a tracer gas can be described by a single exponential [8].

As shown in the Appendix, when the tidal volume, end-expiratory volume, and dead space volume are held constant and when the compartmental flows are synchronous and in the same direction (i.e., no intercompartmental mixing or pendelluft), a sufficient condition for homogeneous distribution of gas concentrations is that

$$\frac{V_i(E) + \lambda_i V_D}{V_i(E) + V_{Ti}} = \frac{V_j(E) + \lambda_j V_D}{V_j(E) + V_{Tj}} \tag{1}$$

for all alveolar compartments $(i, j = 1, 2, \cdots, n)$ taken in pairs. Here, V_{Ti} and $V_i(E)$ are the tidal volume and end-expiratory volume of compartment i, respectively; λ_i is the fraction of the end-expiratory gas volume existing in the common dead space V_D which enters compartment i during the subsequent inspiration. We shall call the ratio given in (1) the generalized dilution index of compartment i, or *GDI*(i). It will be shown that the *GDI*(i) is useful in relating mechanics to gas concentration distribution.

If the $\lambda_i (i = 1, 2, \cdots, n)$ are distributed in the same proportion as the *end-inspiratory* volumes, then (as shown in the Appendix) a sufficient condition for homogeneous gas concentration distribution is that

$$\frac{V_i(E)}{V_i(E) + V_{Ti}} = \frac{V_j(E)}{V_j(E) + V_{Tj}} \tag{2}$$

for all alveolar compartments $(i, j = 1, 2, \cdots, n)$ taken in pairs. We shall call this ratio the simple dilution index of compartment i, or *SDI*(i). As shown later, comparisons between *GDI* and *SDI* provide a useful method for assessing how the distribution of initial dead space gas to the alveolar compartments affects inhomogeneity. A condition equivalent to (2) was suggested by Defares and Donleben [6]:

$$V_{Ti}/V_i(E) = V_{Tj}/V_j(E).$$

A number of investigations (including [5], [6], [13], [14], [18]) have attempted to explain inhomogeneous distribution of gas concentrations in terms of concepts based on linear mechanical models, i.e., unequal time constants. Such efforts have yielded unsatisfying results. For example, Cutillo *et al.* [5] found that a linear, two-compartment model with pendelluft correction was insufficient for predicting multibreath washouts of normals and abnormals at various breathing rates. Problems in such analyses can arise because of the inherent nonlinear nature of the pulmonary system. While the lungs may exhibit uniform mechanical behavior (implying equal mechanical time constants of representative alveolar compartments) at one volume–pressure operating point, they may not do so at another. More importantly, equal time constants inferred for a particular end-expiratory lung volume imply only that the distribution of tidal volume to alveolar compartments is independent of frequency. This condition alone

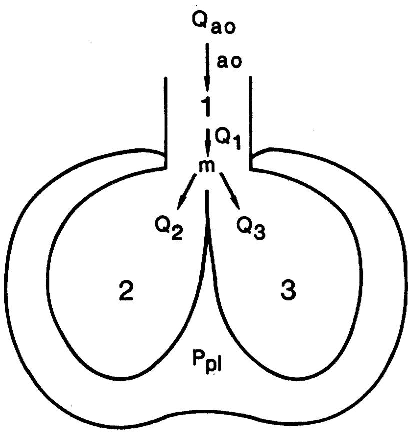

Fig. 1. Model structure with conducting airway {1} and alveolar compartments {2 and 3}. $V_1 = V_D$—the dead space volume.

does not satisfy the requirements of either (1) or (2) for homogeneous gas concentration distribution. In fact, (1) and (2) indicate that it is necessary to know how mechanical abnormalities will alter distributions of regional resting volumes, initial dead space volume, and regional tidal volumes, as well as intercompartmental gas mixing [which is not even accounted for by (1)] at various end-expiratory volumes and breathing rates; hence, the need for a nonlinear model.

Model Development

The lungs are composed of a complex network of branching airways leading to a vast number of gas exchanging alveolar regions. However, the simplest system which is capable of displaying the functional effects of nonuniform mechanics on inhomogeneity requires two parallel, perfectly mixed alveolar compartments connected to a single, constant-volume airway (dead space) in which no mixing occurs (Fig. 1). There is a mixing point m at the junction of the two alveolar compartments and the conducting airway. The model equations derived from mass and force balances describe the intrabreath dynamics of pressure, flow, volume, and gas species concentration after a step change in gas composition at the airway opening.

Mass Balances

Consider a (dry gas) mass balance from the airway opening ao to some point 1 in the dead space (compartment 1). Let Q represent flow rate, where flow into the lung is positive, $Q_{ao} > 0$. For constant density ρ_{ao} and constant dead space volume V_D, the balance equation is

$$\rho_{ao} Q_{ao} = \rho_1 Q_1. \tag{3}$$

(On expiration $\rho_{ao} = \rho_1$, but on inspiration $\rho_{ao} \neq \rho_1$ due to temperature and dry gas partial pressure differences between environmental and respiratory gas.)

For the mixing node m we define flow to be positive when it is directed distally, in which case, the mass balance at node m is

$$-\rho_1 Q_1 + \rho_2 Q_2 + \rho_3 Q_3 = 0.$$

For the breathing patterns of interest, pressure variations are sufficiently small with respect to the absolute pressure so that gas compression can be neglected. Consequently, the mass density is approximately uniform and constant throughout the lung and

$$Q_1 = Q_2 + Q_3. \tag{4}$$

By definition, the volume of the lung V_L is given by

$$V_L = V_D + V_2 + V_3 \tag{5}$$

where V_2 and V_3 are the volumes of compartments 2 and 3, respectively. For constant dead space volume, the time derivative of (5) becomes

$$\dot{V}_L = \dot{V}_2 + \dot{V}_3. \tag{6}$$

For alveolar compartments $i = 2, 3$, we assume negligible net alveolar-capillary transport. Therefore, a mass balance for compartment i is

$$\frac{d}{dt}[\rho_i V_i] = \rho_i Q_i$$

Since the gas density within the lungs is approximately constant at all times, this reduces to

$$\dot{V}_i = Q_i. \tag{7}$$

From (4), (6), and (7), we get

$$\dot{V}_L = Q_1. \tag{8}$$

Mechanics

We assume that the pressure drop from the mixing point (at the distal end of the conducting airway) to the pleural space across each alveolar compartment (Fig. 1) is identical, i.e., $(P_m - P_{pl}) = (P_m - P_{pl})_i$, for $i = 2, 3$. The transpulmonary pressure can then be expressed as the sum of pressure differences over the conducting airway $P_{ao} - P_m$ and the alveolar compartments $P_m - P_{pl}$:

$$P_{tp} = (P_{ao} - P_m) + (P_m - P_{pl}). \tag{9}$$

The extrathoracic airways and intrathoracic airways containing substantial cartilage are rigid compared to the distal airways. Furthermore, we will be considering only low or moderate flow conditions, i.e., small tidal volumes (compared to end-expiratory volume) and low breathing frequencies ($\leqslant 1.0$ Hz). Hence, these airways can be represented as having a constant volume with a linear pressure flow relation. That is,

$$(P_{ao} - P_m) = R_1 Q_1 = R_1 \dot{V}_L, \tag{10}$$

where R_1 is a resistance coefficient for the conducting airway.

The pressure drop $(P_m - P_{pl})$ across each alveolar compartment is due to both dissipation and storage of energy. This can be expressed as

$$(P_m - P_{pl}) = f_i(V_i, \dot{V}_i) + g_i(V_i) \tag{11}$$

in which the function $f(V_i, \dot{V}_i)$ is the pressure drop associated with dissipation at the inlet to the compartment (i.e., the peripheral airway) and $g(V_i)$ is the pressure drop associated with elastic properties of the alveolar tissue. Unlike the conducting airways, the peripheral airways associated with the alveolar compartments are embedded in the lung parenchyma and their lumen dimensions depend upon radial forces from surrounding tissue. Consequently, their flow-related energy dissipation will be affected as volume changes. Specifically, we assume that the pressure drop along the peripheral airways is inversely proportional to the volume of the related alveolar compartment:

$$f_i(V_i, \dot{V}_i) = (b_i/V_i)\dot{V}_i \tag{12}$$

where b_i is a specific resistance for compartments $i = 2, 3$.

The elastic properties which cause energy to be stored are found from a "static" pressure-volume curve. We assume that the system operates around some tidal volume on the nonlinear deflation curve such that static hysteresis is negligible. Since an exponential expression is an appropriate constitutive equation to describe the elastic behavior of the lung parenchyma [17], it provides a reasonable form for the energy storage component of the pressure drop:

$$g(V_i) = h_i \exp(V_i/\epsilon_i) \tag{13}$$

where h_i is a pressure coefficient and ϵ_i is a volume coefficient for compartments $i = 2, 3$.

Equations (12) and (13) are combined to give the complete expression for the pressure drop across each alveolar compartment:

$$P_m - P_{pl} = (b_i/V_i)\dot{V}_i + h_i \exp(V_i/\epsilon_i). \tag{14}$$

Substitution of (10) and (14) into (9) gives us the net transpulmonary pressure difference:

$$P_{tp} = R_1 \dot{V}_L + (b_i/V_i)\dot{V}_i + h_i \exp(V_i/\epsilon_i). \tag{15}$$

Inertial terms have been excluded from (15). Because we are interested in the system's behavior for relatively small tidal volumes and low frequencies, the gas and tissues of the respiratory system have small inertance. For simulations, transpulmonary pressure is the input-forcing function causing flow into or out of compartments. Using (6) and rearranging (15), we get for $i, j = 2, 3$ and $i \neq j$

$$\dot{V}_i = \left(\frac{V_i}{V_i R_1 + b_i}\right)[-R_1 \dot{V}_j - h_i \exp(V_i/\epsilon_i) + P_{tp}]. \tag{16}$$

Species Gas Transport

Consider the species transport equations of an inert, insoluble tracer gas. We neglect axial dispersion because the dominant contribution to gas concentration inhomogeneity during tidal breathing is associated with differences in parallel lung units. Hence, in the dead space, we assume plug transport occurs, which means that the transport of an incremental volume of gas species between the airway opening and mixing point is characterized by a pure time delay. The gas that enters the airway opening during inspiration will reach the mixing point after the dead space is cleared. For the first breath,

$$C_{1m} = \begin{Bmatrix} C(0) \\ C_{in} \end{Bmatrix} \quad \text{for} \quad |v_L| \begin{Bmatrix} < \\ > \end{Bmatrix} V_D$$

where C_{1m} is the species concentration of gas entering the mixing node from the dead space, $C(0)$ is the initial concentration throughout the lung, C_{in} is the input concentration, and v_L is the change in lung volume from the beginning of an inspiration (or expiration).

If, on inspiration, the dead space had been cleared by the inspired gas, then, at the beginning of expiration, the species concentration throughout the dead space is the input concentration C_{in}. Consequently, during expiration, until the dead space is cleared, the output concentration at the airway opening C_{ao} is the input concentration

$$C_{ao}(t) = \begin{Bmatrix} C_{in} \\ C_m(t - \theta_k) \end{Bmatrix} \quad \text{for} \quad |v_L| \begin{Bmatrix} < \\ > \end{Bmatrix} V_D$$

where the dead space clearance time θ_j for any incremental volume of gas entering the dead space at any time t_j during expiration (or inspiration) is defined by

$$\left| \int_{t_j}^{\theta_j + t_j} Q_1 \, dt \right| = V_D.$$

Because the flow rate is not constant, the clearance time θ_j is not constant.

The mechanical state of the system may be such that ventilation of both alveolar compartments is not in synchrony or in the same direction; hence, pendelluft occurs. There are six possible directions of flows among the conducting airway and alveolar compartments. Consequently, the general form of the species molar balance at the mixing node must be carefully written to account for all cases:

$$\begin{aligned} 0 = &-Q_1 [C_m u(-Q_1) + C_{1m} u(Q_1)] \\ &+ Q_2 [C_m u(Q_2) + C_2 u(-Q_2)] \\ &+ Q_3 [C_m u(Q_3) + C_3 u(-Q_3)] \end{aligned} \tag{17}$$

where C_m is the species molar concentration of the gas leaving the mixing node m, C_2 and C_3 are the species molar concentrations in compartments 2 and 3, respectively, and $Q_i > 0$ when flow is directed distally. The unit step function is defined as

$$u(Q) = \begin{Bmatrix} 1 \\ 0 \end{Bmatrix} \quad \text{for} \quad Q \begin{Bmatrix} > \\ < \end{Bmatrix} 0.$$

From this equation, we can solve for C_m regardless of the flow directions.

The general form of the species molar balance for alveolar compartment i ($i = 2, 3$) with negligible alveolar-capillary transport is

$$\frac{dC_i V_i}{dt} = Q_i [C_m u(Q_i) + C_i u(-Q_i)]. \tag{18}$$

Combining equations (7) and (18), we get

$$V_i \frac{dC_i}{dt} = Q_i [C_m - C_i) u(Q_i)]. \tag{19}$$

We see that on inspiration ($Q_i > 0$)

$$\frac{dC_i}{dt} = \frac{Q_i}{V_i}(C_m - C_i)$$

and on expiration ($Q_i < 0$)

$$\frac{dC_i}{dt} = 0 \Rightarrow C_i = \text{constant}.$$

Note that the analysis of the washout of an insoluble gas does not introduce any additional model parameters beyond those which arise from the mechanical equations.

Parameter Values for Simulations

As a reference for model simulations, we chose a pulmonary system with identical alveolar compartments and "normal" values for its linearized mechanical parameters. We assume an initial lung volume $V_L = 3.15$ l and a dead space volume $V_D = 0.15$ l. Thus, the volume of each alveolar compartment $i = 2, 3$ is $V_i = 1.5$ l. These initial volume estimates (which differ from the compartmental volumes during steady-state breathing) are used to compute approximate values of the mechanical parameters.

A total airway resistance $R_{taw} = 1.6$ cm H_2O/l/s and a total pulmonary resistance $R_{tp} = 1.9$ cm H_2O/l/s are typical in normal man [4]. Macklem and Mead [11] reported that the peripheral airways accounted for about 0–20 percent of R_{taw} over the vital capacity. We assume 85 percent of R_{taw} is associated with conducting airways, that is $R_c = 1.36$ cm H_2O/l/s. Furthermore, we assume the differences between total pulmonary resistance and total airway resistance can all be assigned to the energy dissipation term of the alveolar compartment. Consequently, the total peripheral resistance is $R_p = 0.54$ cm H_2O/l/s. If R_p is uniformly distributed between the two parallel alveolar compartments, then in terms of a linear model, $(R_p)_i = 2R_p = 1.08$, for $i = 2, 3$. For the pressure-flow relation of the conducting airway (10), R_c is an obvious choice for a typical R_1. In the pressure-flow relation of alveolar compartments $i = 2, 3$ in (12), we make the approximation $b_i = V_i(E)(R_p)_i = (1.5)(1.08) = 1.62$.

A typical lung compliance is $C_L = 0.2$ l/cm H_2O [4]. If the elastic properties are uniformly distributed between two parallel alveolar compartments of equal volume, then in terms of a linear model, $C_2 = C_3 = C_L/2 = 0.1$ l/cm H_2O. If we assume that the static transpulmonary pressure varies from 5 cm H_2O to 9 cm H_2O during inspiration, then the volume increase in each compartment would be 0.4 l. We use this information to obtain reference values of ϵ_i and h_i from (13). Assuming that each alveolar compartment has an end-expiratory volume of 1.5 l and an end-inspiratory volume of 1.9 l, we see that

$$\left.\begin{array}{l} 5 = h_i \exp\,[1.5/\epsilon_i] \\ 9 = h_i \exp\,[1.9/\epsilon_i] \end{array}\right\} \Rightarrow h_i = 0.552,\ \epsilon_i = 0.68.$$

As a check on this procedure, we linearize (13) using a Taylor series expansion about any point V_i^o:

$$g(V_i) = (h_i/\epsilon_i) \exp\,(V_i^o/\epsilon_i)]\,[V_i - V_i^o] = (1/C_i)[V_i - V_i^o]. \tag{20}$$

Taking $V_i^o = 1.7$ l to be the midvolume point in the tidal volume range, and using the above parameter values, (20) yields a compliance of 0.10 l/cm H_2O.

SIMULATION RESULTS

An understanding of this model requires that we examine its behavior under a variety of conditions that simulate experimental studies of normal and abnormal lungs. The simulations explore two areas:

1) effects of pulmonary mechanical parameters, and

2) effects of volume operating point and breathing frequency.

For these simulations, one must choose forcing functions (transpulmonary pressure) and parameter values which allow simulation of normal lung behavior and various types of abnormal behavior. The equations governing pulmonary mechanics are solved by computer to obtain the (nontransient) strictly periodic volume and flow dynamics. For this "steady state," equations for species dynamics are solved concurrently with those for mechanics to simulate a multibreath N_2 washout experiment. The numerical solution uses a 4th-order Runge-Kutta algorithm with a sufficiently small step size to guarantee accuracy.

Effects of Pulmonary Mechanical Parameters

If the model is forced by an invariant transpulmonary pressure wave shape, then changes in the pulmonary mechanical parameters will alter several measurable variables: tidal volume V_T, end-expiratory lung volume $V_L(E)$, and the end-expiratory species (N_2) concentration at the airway opening $C_{ao}(k)$, at the end of breath k. The species concentration at the airway opening normalized with respect to the initial concentration within the lungs is defined as $Y(k) = C_{ao}(k)/C(0)$. Furthermore, variables that are associated with each compartment but not measurable can be computed from the model to characterize the effects of changes in mechanical parameters. The pendelluft volume fraction, a measure introduced by Otis *et al.* [13], indicates asynchronous ventilation:

$$V_P/V_T = [(V_{T2} + V_{T3})/V_T] - 1.$$

For fixed tidal volume, this fraction increases as the volume of pendelluft increases. Inhomogeneous gas concentration distribution is indicated by the difference between gas species concentrations in the alveolar compartments at the end of breath k:

$$\Delta X(k) = |X_2(k) - X_3(k)|$$

where the normalized concentration in compartment i is defined as $X_i(k) = C_i(k)/C(0)$. As shown in the Appendix, for any case in which asynchronous flow is negligible, $X_i(1) = GDI(i)$ and $\Delta GDI = |GDI(2) - GDI(3)| = \Delta X(1)$. If the initial gas volume in the dead space is distributed to the alveolar compartments in the same proportion as their end-inspiratory volumes, i.e., (A4) holds, then $\Delta SDI = |SDI(2) - SDI(3)| = \Delta GDI = \Delta X(1)$.

In Table I, parameter values are given for six cases. Case 1 represents a normal (uniform) lung and Case 6 represents an

TABLE I
PARAMETER VALUES USED IN SIMULATIONS

PARAMETERS		CASE 1	CASE 2	CASE 3	CASE 4	CASE 5	CASE 6
Resistance Coefficient for Conducting Airway (cm H_2O/L)	R_1	1.36	2.72	1.36	1.36	1.36	1.36
Specific Resistances of Compartments (cm H_2O-sec)	b_2	1.62	1.62	1.62	1.62	1.62	1.62
	b_3	1.62	1.62	1.62	1.62	20.00	25.00
Compartmental Volume Coefficients (L)	ϵ_2	0.68	0.68	0.68	0.68	0.68	0.68
	ϵ_3	0.68	0.68	1.57	0.68	0.68	2.05
Compartmental Pressure Coefficients (cm H_2O)	h_2	0.552	0.552	0.552	0.552	0.552	0.552
	h_3	0.552	0.552	0.552	2.000	0.552	2.400

obstructive (nonuniform) lung. A distinctive variation of each parameter ($R_1, \epsilon_i, h_i, b_i$) is given in Cases 2, 3, 4, and 5.

To simulate the effects of parameter values on model behavior, we used a periodic transpulmonary forcing function that has an exponential rise on inspiration and fall on expiration. Specifically, for any breath k, where $t_0(k)$ and $t_1(k)$ are the times at which inspiration and expiration start, respectively, we let

$$P_{tp} = P(0) + A \begin{cases} 1 - \exp\{-[t - t_0(k)]/\tau_R\}, & t_0(k) \leqslant t \leqslant t_1(k) \\ \exp\{-[t - t_1(k)]/\tau_F\}, & t_1(k) \leqslant t \leqslant t_0(k+1) \end{cases}$$

The parameter values are $P(0) = 5$ cm H_2O, $A = 4$ cm H_2O, $2\tau_R = \tau_F = 0.22$ s, and the rise time is half the fall time, i.e., $[t_0(k+1) - t_1(k)] = 2[t_1(k) - t_0(k)] = 2.67$ s. The breathing rate is 0.25/s.

Case 1: The reference lung is taken to be uniform. Fig. 2 and Table II show the flow, volume, and species (N_2) concentration dynamics and performance characteristics for this case. The alveolar compartmental volumes and concentrations are identical at all times. During inspiration, the species concentrations X_i in the alveolar compartments remain constant until the dead space is cleared. Following this, mixing occurs with the inspired gas which contains no N_2, and the compartmental species concentrations decrease. During each expiration, output N_2 concentration at the airway opening is zero until the dead space is cleared, and then rises to the constant value present in both alveolar compartments.

Case 2: Increasing the conducting airway resistance coefficient R_1 causes an increase in the flow-related pressure drop along the conducting airway. Since the forcing function was unchanged from Case 1, this leads to a decrease in the flows to the alveolar compartments and a decrease in tidal volume for the whole lung (Table II). Both the pendelluft fraction and the generalized dilution index difference between compartments ΔGDI are zero, so that mechanical behavior is uniform and gas concentration distribution remains homogeneous.

Case 3: Increasing the volume coefficient ϵ_3 has the effect on the pressure-volume characteristics of the lung shown in Fig. 3. In particular, compartment 3 is less stiff so that at a given pressure the volume is higher and for a given change in

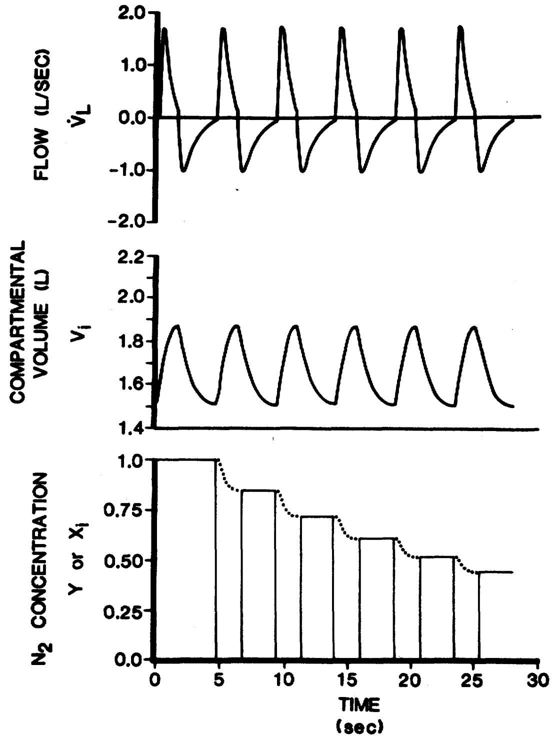

Fig. 2. Flow, volume, and concentration dynamics during multibreath N_2 washout for uniform (normal) model (Case 1, Table I)—flow at airway opening $\dot V_L$, alveolar compartment volumes $V_i (i = 2, 3)$, normalized N_2 concentrations at airway opening Y, and in alveolar compartments $X_i (i = 2, 3)$. The alveolar compartment outputs are identical. On inspiration, X_i is shown as the dotted line and is distinct from Y, shown as a solid line.

pressure the change in volume is larger than in Case 1. These shifts in compartmental resting and tidal volumes have two effects on compartment 3: 1) The linearized compliance increases, and 2) the compartmental resistance decreases. Nevertheless, the compartmental time constants remain essentially equal (Table III). Consequently, the compartmental flows are synchronous so that the pendelluft volume fraction is zero. The initial gas in the dead space is distributed to the alveolar compartments in essentially the same proportion as their end-inspiratory volumes (as given by (A4) in the Appendix). Both the tidal volume and end-expiratory volume of compartment 3 increase in a way such that $GDI(2) = GDI(3)$ [or $SDI(2) = SDI(3)$]. Hence, as expected from (A3) or (A6), gas concentration distribution remains homogeneous (i.e., the normalized concentration difference $\Delta X(1) = 0$). (Through simulations we have found that whenever $b_2 = b_3$ and $h_2 = h_3$, changes in ϵ_3 do not cause nonuniform mechanical behavior or inhomogeneous gas concentration distribution.)

Case 4: Increasing the pressure coefficient h_3 shifts the entire pressure-volume curve downward (Fig. 3). That is, for the same P_{tp} as in Case 1, compartment 3 has a smaller end-expiratory volume. However, its tidal volume changes little compared to Case 1, and consequently, its effective compliance (Table III) is not significantly altered. An increase in the mechanical time constant of compartment 3 is caused by the increase of its compartmental resistance. Nevertheless, at a breathing rate of 0.25/s the difference in compartmental time constants was not large enough to cause the asynchronous

TABLE II
PERFORMANCE CHARACTERISTICS OF CASES 1–6 (TABLE I) FOR SIMULATIONS WITH A PIECEWISE EXPONENTIAL PRESSURE FORCING FUNCTION

	End-Expiratory Volumes (L)			Tidal Volumes (L)			End-Inspiratory Volume Ratio	Dead Space Gas Distribution Ratio	Simple Dilution Index Difference	Generalized Dilution Index		Pendelluft Fraction	Normalized End-Expiratory Species Fraction		
CASE	$V_L(E)$	$V_2(E)$	$V_3(E)$	V_T	V_{T2}	V_{T3}	$\frac{V_2(E)+V_{T2}}{V_3(E)+V_{T3}}$	λ_2/λ_3	ΔSDI	GDI(2)	GDI(3)	V_P/V_T	Y(1)	$X_2(1)$	$X_3(1)$
1	3.16	1.50	1.50	.754	.377	.377	1.00	1.00	0.00	.84	.84	0.00	.84	.84	.84
2	3.21	1.53	1.53	.638	.319	.319	1.00	1.00	0.00	.87	.87	0.00	.88	.88	.88
3	5.20	1.52	3.52	1.130	.340	.791	0.43	0.47	0.00	.84	.84	0.00	.85	.85	.85
4	2.30	1.51	0.64	.734	.372	.363	1.88	1.82	0.16	.85	.69	0.00	.78	.87	.71
5	3.25	1.51	1.59	.530	.366	.184	1.06	8.09	0.09	.88	.91	0.04	.91	.89	.91
6	3.62	1.52	1.95	.513	.358	.195	0.88	31.26	0.10	.87	.91	0.08	.91	.90	.93

Note: V_D = 0.15 l in all cases.

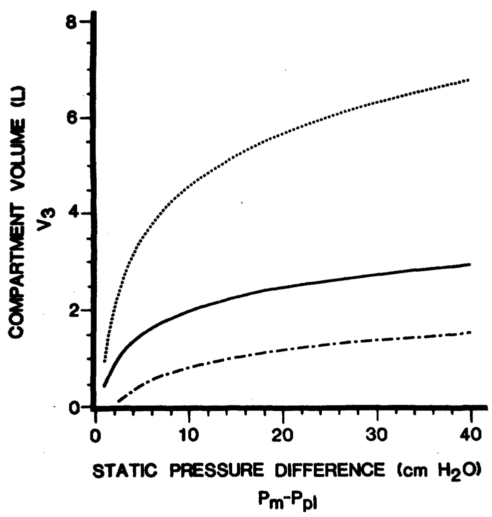

Fig. 3. Effect of pressure and volume coefficients (h_3 and ϵ_3) on the static pressure-volume curve for compartment 3. With respect to Case 1 (solid line), Case 3 (dotted line) has an increased ϵ_3 and Case 4 (dashed line) has an increased h_3. The parameter values are given in Table I.

TABLE III
EFFECTIVE LINEARIZED MECHANICAL PARAMETERS FOR CASES 1–6 (TABLE I) WITH PIECEWISE EXPONENTIAL PRESSURE FORCING FUNCTION AND VOLUME OPERATING POINTS GIVEN IN TABLE II

Case	R_2	R_3	C_2	C_3	T_2	T_3
1	1.08	1.08	.101	.101	0.109	0.109
2	1.06	1.06	.102	.102	0.108	0.108
3	1.07	0.46	.102	.232	0.109	0.107
4	1.07	2.53	.100	.100	0.107	0.253
5	1.07	12.58	.101	.104	0.108	1.308
6	1.07	12.82	.100	.314	0.107	4.025

The alveolar compartmental resistances are $R_i = b_i/V_i(E)$, where $V_i(E)$ is the end-expiratory volume of compartment i (as shown in Table II). The alveolar compartmental compliances are $C_i = \Delta V_i/\Delta P_i$, where $\Delta V_i = V_{Ti}$ is the compartmental tidal volume and ΔP_i is the corresponding change in transpulmonary pressure as defined by (13). The mechanical time constants are $T_i = R_i C_i$.

flow to be reflected in the pendelluft fraction ($V_P/V_T = 0$). Thus, even though the mechanical parameters of compartments 2 and 3 are not the same, the system behaves as though it were mechanically uniform under the specified operating conditions. The distribution of the initial dead space gas to the alveolar compartments is essentially the same as that of the end-inspiratory volumes. However, because the end-expiratory volume of compartment 3 is much smaller than that of compartment 2 and their tidal volumes are about the same, we see from Table II that $\Delta SDI \approx \Delta GDI \approx \Delta X(1)$ is substantially different from zero (i.e., there is significant inhomogeneity).

Case 5: Increasing the resistance coefficient b_3 increases the flow-related pressure drop in compartment 3. As shown in Table III, the mechanical time constant of compartment 3 is greater than that of compartment 2; this is reflected in a significant pendelluft fraction (Table II). The increase in b_3 produces a major decrease in the tidal volume and a slight increase in the end-expiratory volume of compartment 3. Furthermore, during inspiration the initial gas volume in the dead space is not distributed to the alveolar compartments in the same proportion as their end-inspiratory volumes (i.e., (A4) does not hold). Consequently, ΔSDI [or (A6)] cannot be used to calculate $\Delta X(1)$; in fact, ΔSDI is much higher than $\Delta X(1)$, while ΔGDI is nearly equal to it [as expected from (A3)].

Case 6: A nonuniform, obstructive lung is simulated by increasing b_3, h_3, and ϵ_3 (Table I) such that the values of linearized resistance and compliance of compartment 3 are higher than in the reference Case 1 (Table III). This causes the mechanical time constant of compartment 3 to be much

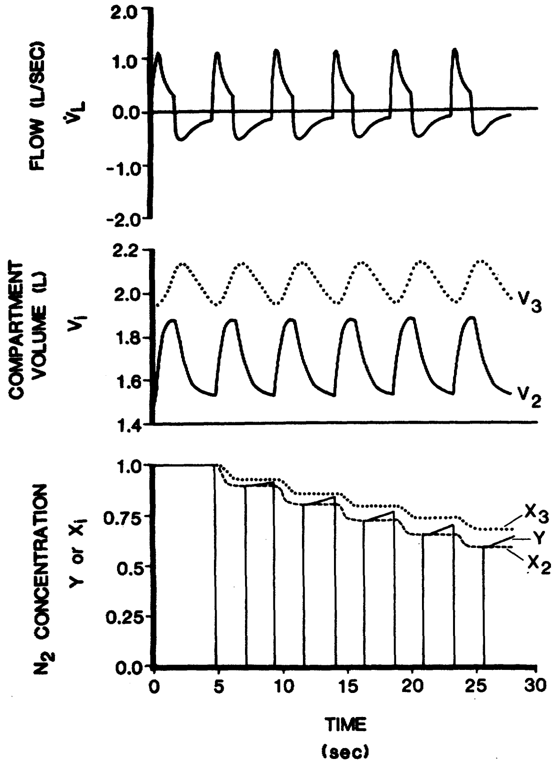

Fig. 4. Flow, volume, and concentration dynamics during multibreath N_2 washout for nonuniform (obstructive) model (Case 6, Table I)—flow at airway opening $\dot{V}_L$, alveolar compartment volumes $V_i (i = 2, 3)$, normalized N_2 concentrations at airway opening Y, and in alveolar compartments $X_i (i = 2, 3)$.

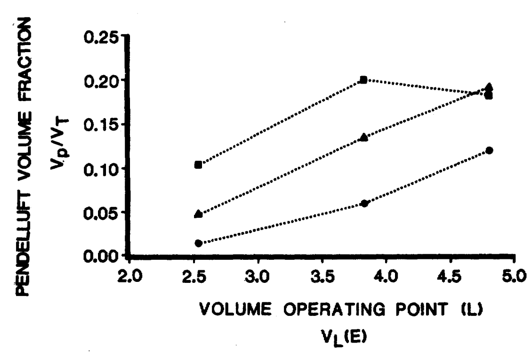

Fig. 5. Pendelluft fraction $V_P/V_T = [(V_{T2} + V_{T3})/V_T] - 1$ versus volume operating point at three breathing frequencies: 0.25 Hz (squares), 0.5 Hz (triangles), and 1.0 Hz (circles). Nonuniform model (Case 6, Table I).

TABLE IV
MEAN EFFECTIVE LINEARIZED MECHANICAL PARAMETERS FOR CASE 6 (TABLE I) USING A SINUSOIDAL PRESSURE FORCING FUNCTION AT VARIOUS VOLUME OPERATING POINTS

V_L(E) Liters	R_2	R_3	C_2	C_3	T_2	T_3
4.81	0.90	8.80	.068	.206	0.060	1.85
3.83	1.06	11.74	.099	.294	0.104	3.50
2.54	1.37	20.50	.158	.467	0.216	9.88

larger than that of compartment 2 and the resulting asynchronous compartmental flows produce a sizeable pendelluft fraction. Fig. 4 shows the flow, volume, and species concentration dynamics. From Table II and Fig. 4 we see that compartment 3 has an increased end-expiratory volume and decreased tidal volume. This causes the values of X_2 to always be less than X_3 (Fig. 4). Here, the end-inspiratory volume ratio is much different than the dead space gas distribution ratio. Again, ΔSDI is much larger than $\Delta X(1)$, while ΔGDI is nearly equal to $\Delta X(1)$. Furthermore, because of the asynchronous flows, compartment 2, with $X_2 < X_3$, empties first during expiration and a distinct rising alveolar plateau occurs at the airway opening for each breath. The slope of the plateau on successive breaths changes with the difference in compartmental concentrations.

Effects of Operating Point and Frequency

A comparison of uniform and nonuniform behavior (Cases 1 and 6) during breathing is inadequate if changes in volume operating point and frequency are not considered. To evaluate the effects of these two parameters, we chose to simulate the transpulmonary pressure forcing function as a sinusoid:

$$P_{tp} = P(0) + A[1 - \cos(2\pi f t)].$$

The values of $P(0) = 5$ cm H_2O and $A = 2$ cm H_2O were chosen for the uniform (Case 1) and nonuniform (Case 6) models to establish a reference tidal volume V_T and volume operating point (end-expiratory lung volume) $V_L(E)$ at a breathing frequency $f = 0.25$ Hz. At higher frequencies (0.5 and 1.0 Hz), the values of $P(0)$ and A were empirically adjusted so that V_T and $V_L(E)$ remained within 5 percent of their original values. This procedure was repeated at volume operating points above and below the reference end-expiratory volume and with the same reference tidal volume V_T.

The dependence of the model on operating point and frequency is evident from the pendelluft volume fraction V_P/V_T, the simple and generalized dilution index differences ΔSDI and ΔGDI, respectively, and compartmental concentration differences $\Delta X(k)$ during a multibreath washout experiment. These indexes are computed from nonmeasurable compartmental variables. For the uniform model, V_P/V_T is zero under all conditions. For the nonuniform model, V_P/V_T can increase or decrease with changes in $V_L(E)$ or breathing frequency as shown in Fig. 5. Furthermore, the effective linearized mechanical properties of both compartments change significantly with changes in $V_L(E)$ (Table IV).

Differences in compartmental dilution indexes ΔSDI and ΔGDI are each approximations to the simulated normalized intercompartmental concentration differences on the first breath of a washout $\Delta X(1)$ [(A3) and (A6)]. Fig. 6 shows ΔSDI and ΔGDI versus $\Delta X(1)$ for Case 6 at several breathing frequencies and volume operating points. Because Case 6 exhibits asynchronous compartmental flows, the simulated concentration differences will be affected by both the nonuniform distribution of the initial dead space gas to the compartments as well as the intercompartmental gas mixing (or pendelluft). Neither of these phenomena is properly accounted for by the simple dilution index. In fact, ΔSDI values are always larger than those of the simulated $\Delta X(1)$. The

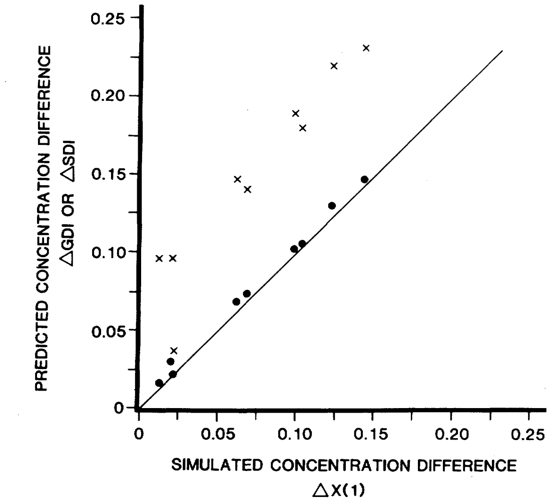

Fig. 6. Normalized intercompartmental concentration differences predicted by both the simple dilution index difference, ΔSDI(XXX), and the generalized dilution index difference, ΔGDI(●●●) versus simulated concentration differences $\Delta X(1)$ at the end of the first breath for nonuniform model (Case 6, Table I) at several breathing frequencies and operating points. The solid line is the line of identity.

ΔGDI, which does account for the intercompartmental distribution of initial dead space gas but not asynchronous compartmental flows, exhibits values much closer to $\Delta X(1)$.

The intercompartmental gas concentration distribution can be characterized by the difference between end-tidal, normalized, compartmental species concentrations during a multibreath N_2 washout. To characterize washouts performed at several breathing frequencies and volume operating points, we will use the mean value of this difference (listed in Table V):

$$\overline{\Delta X} = \sum_{k=1}^{N} |X_2(\eta_k) - X_3(\eta_k)|/N = \sum_{k=1}^{N} \Delta X(k)/N$$

where N is the number of breaths at which the dilution number $\eta_k = 8$. For the special case of a constant breathing pattern, $\eta_k = kV_T/V_L(E)$. Use of the dilution number minimizes the effects of variable tidal volume and end-expiratory volume [16]. Our claim is that $\overline{\Delta X}$ increases with the inhomogeneity of gas concentration distribution over the washout.

Indexes which can be evaluated experimentally are also obtained from the model output. Assessment of nonuniform mechanical function is given by the variation of dynamic compliance C_d with frequency. We estimate C_d as the ratio $V_T/[P_{tp}(t_2) - P_{tp}(t_1)]$ computed at successive instants (t_1 and t_2) when flow is zero at the airway opening. As shown in Fig. 7(a), C_d of the uniform model does not change with increasing frequency, but decreases significantly as $V_L(E)$ increases. For the nonuniform model [Fig. 7(b)], C_d decreases with both frequency and $V_L(E)$. The decrease in C_d with frequency is less for larger $V_L(E)$, i.e., at a larger volume operating point, the system acts more uniformly.

A measurable variable that directly reflects the intrapulmonary gas concentration distribution is the N_2 concentration at the airway opening C_{ao}. The normalized N_2 concentrations $Y(k)$ observed at the end of successive expirations

TABLE V
INDEX OF INHOMOGENEITY ($\overline{\Delta X}$) FOR CASE 6 USING A SINUSOIDAL TRANSPULMONARY PRESSURE FORCING FUNCTION AT SEVERAL FREQUENCIES AND VOLUME OPERATING POINTS

End-Expiratory Volume $V_L(E)$ (Liters)	Frequency (Hz)	Mean End-Tidal Concentration Difference, $\overline{\Delta X}$
2.54	1.00	.470
2.54	0.50	.321
3.83	1.00	.291
2.54	0.25	.167
4.81	1.00	.162
3.83	0.50	.126
4.81	0.50	.036
4.81	0.25	.033
3.83	0.25	.018

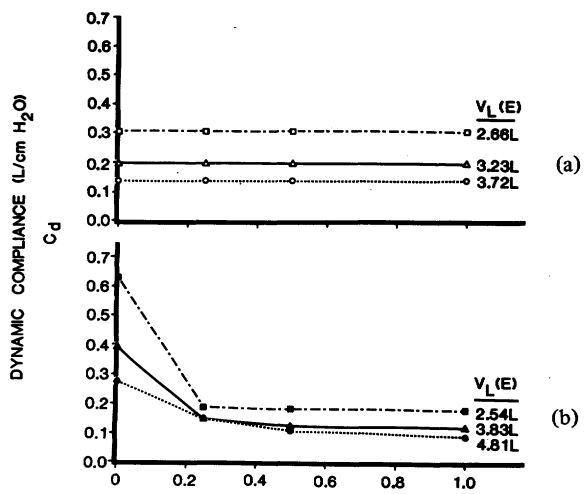

Fig. 7. Effects of breathing frequency and volume operating point on total pulmonary dynamic compliance C_d. (a) Uniform model (Case 1, Table I). (b) Nonuniform model (Case 6, Table I).

($k = 1, 2, \cdots$) during an N_2 washout characterize the extent of inhomogeneity. For a constant V_T, when intercompartmental concentration differences are negligible, this model would show that $Y(k)$ decreases as a single exponential (or linearly on a semilog plot) with breath number k or dilution number η_k for any breathing frequency or volume operating point. The less homogeneous the compartmental concentration distribution, the more these relationships deviate from a single exponential. Curves of $Y(\eta_k)$ are shown in Fig. 8 for the nonuniform model (Case 6) at frequencies of 0.25 and 1 Hz for the three values of $V_L(E)$. Although some of these washout curves appear linear for some frequencies and volume operating points, the nonlinearity is evident in others. At each $V_L(E)$, increasing the breathing frequency resulted in a more nonlinear washout curve.

A useful index of inhomogeneity obtained from the washout

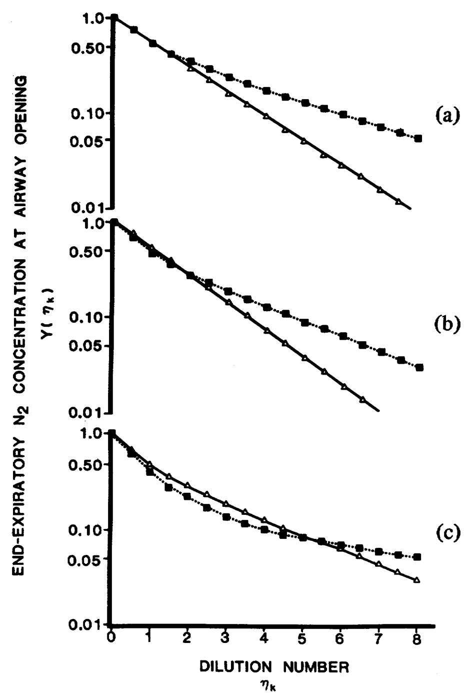

Fig. 8. Multibreath N_2 washout of nonuniform model (Case 6, Table I) at 0.25 Hz (triangles) and 1.0 Hz (squares) for different volume operating points $V_L(E)$. (a) 4.81 l, (b) 3.83 l, and (c) 2.54 l. The washouts at 0.5 Hz for each $V_L(E)$ fall between those shown for 0.25 and 1.0 Hz. To avoid cluttering the figure they are not shown.

$Y(\eta_k)$ is given by the mean dilution number μ_1/μ_0 [7], [16], in which the rth moment of $Y(\eta_k)$ is

$$\mu_r = \sum_{k=0}^{N} \eta_k^r Y(\eta_k)[\eta_k - \eta_{k-1}) \qquad r = 0, 1, \cdots$$

and $k = N$ when $\eta_k \geqslant 8$. From the definition of η_k for constant breathing pattern, the moments can be computed as

$$\mu_r = [V_T/V_L(E)]^{r+1} \sum_{k=0}^{N} k^r Y(k).$$

The mean dilution number for the uniform and nonuniform cases are shown in Fig. 9 for the same frequencies and operating points as in Figs. 5-7. For the uniform model, the mean dilution number is small and nearly constant under all conditions. At each $V_L(E)$ for the nonuniform model, the mean dilution number tends to increase as frequency increases.

Discussion

The behavior of the pulmonary mechanical system depends directly upon the mechanical parameters and the pressure forcing function to which it is subjected. This model shows that changes in either of these will affect the distribution of four mechanical variables: compartmental resting volumes $V_i(E)$, compartmental tidal volumes V_{Ti}, fraction of initial gas volume in the dead space entering each alveolar compartment λ_i, and the pendelluft fraction V_p/V_T. Furthermore, it demonstrates *how* the distribution of each of these mechanical

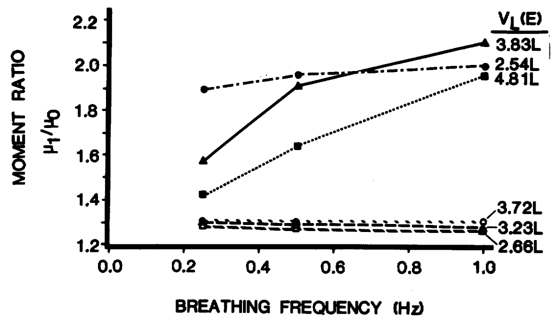

Fig. 9. Effects of breathing frequency and volume operating point on the mean dilution number or moment ratio μ_1/μ_0 of the multibreath N_2 washout. Simulation results for nonuniform (Case 6, Table I closed symbols) and uniform (Case 1, Table I open symbols) models.

variables acts to uniquely determine the distribution of gas concentration throughout the lung as indicated by $\Delta X(1)$, $\overline{\Delta X}$, $Y(k)$, and μ_1/μ_0. Finally, the model indicates that a useful way to interpret the relative importance of these mechanical variables on the gas concentration distribution is to compare the ΔSDI and ΔGDI to $\Delta X(1)$ and $\overline{\Delta X}$.

Uniform Mechanical Behavior

Tables II and III list the effects of altering the mechanical parameters in the manner indicated in Table I while keeping the forcing function the same. When the corresponding parameters are equal in the alveolar compartments, as in Cases 1 and 2, the mechanical variables $V_i(E)$, V_{Ti}, and λ_i are distributed equally between compartments and compartmental flows are synchronous ($V_p/V_T = 0$). Consequently, the system is mechanically uniform and gas concentration distribution is always homogeneous. In Case 3 we see that altering the volume coefficient of compartment 3, ϵ_3, changes its effective resistance and compliance. Nevertheless, the linearized mechanical time constants are equal so that flows are synchronous. The λ_i/λ_j ratio is close to the corresponding ratio of end-inspiratory volumes but the $V_{T2} \neq V_{T3}$ and $V_2(E) \neq V_3(E)$. However, their distribution is such that $GDI(2) = GDI(3)$ [and $SDI(2) = SDI(3)$]; thus, homogeneous gas concentration distribution is maintained. In Case 4, changing the pressure coefficient h_3 of compartment 3 alters its effective resistance and produces unequal mechanical time constants of the compartments. At the simulated breathing rate, this difference is not large enough to produce asynchronous flows or a significant difference between the λ_i/λ_j ratio and the ratio of end-inspiratory volumes. However, since the V_{Ti} are essentially the same while nearly a 4-fold difference in the $V_i(E)$ occurs, there is a large difference in compartmental dilution indexes (e.g., ΔGDI or ΔSDI) and, hence, end-tidal compartmental concentrations $X_i(1)$.

Nonuniform Mechanical Behavior: The Effects of Dead Space and Pendelluft

Unlike Cases 3 and 4, Cases 5 and 6 are both mechanically nonuniform. That is, the parameter changes produce time constant differences substantially larger than that in Case 4, resulting in an appreciable pendelluft fraction. Furthermore, the distribution of the initial dead space gas to the alveolar compartments (λ_i/λ_j) is no longer equal to that of the corresponding ratio of end-inspiratory volumes. In fact, if we do not account for the distribution of the initial dead space gas in assessing the inhomogeneity of gas concentration distribution (i.e., if we use the ΔSDI as a predictor of intercompartmental concentration difference), we would largely overestimate the value of $\Delta X(1)$. However, if we do account for it (i.e., if we use ΔGDI), the estimate is much closer. The implication is that the initial dead space gas is now distributed to the compartments in a way which tends to minimize the compartmental concentration difference.

This last point is substantiated further by Fig. 6. Here we see that for a nonuniform obstructed lung ΔSDI is a very poor indicator of gas concentration distribution (i.e., $\Delta X(1)$) at a particular breathing rate and volume operating point. However, ΔGDI does predict the simulated $\Delta X(1)$ very well. Since the ΔSDI for all washouts are much higher than the ΔGDI, we conclude that in the obstructed lung of Case 6, the dead space is distributed to the alveolar compartments in a way that minimizes the inhomogeneity of gas concentration distribution caused by the nonuniform mechanics. To explain this phenomena, we note that for all washouts the unobstructed compartment has a larger V_{Ti} and smaller $V_i(E)$ than the obstructed one (as indicated by Table II for an exponential forcing function at 0.25/s). However, the tidal volume of the unobstructed compartment receives nearly all of the initial dead space gas which has low oxygen content. Consequently, a significant portion of the tidal volume does not aid in reducing the N_2 concentration of that compartment. On the other hand, the smaller tidal volume of the obstructed compartment is composed almost entirely of inspired air which is 100 percent O_2 so that nearly its entire tidal volume is useful in reducing the N_2 concentration.

Although pendelluft occurs during model simulations (Fig. 5), it is not accounted for by ΔGDI. From Fig. 6 we see that the ΔGDI are close to the simulated $\Delta X(1)$, but consistently larger. This implies that while the effect of pendelluft may not be large, it also tends to reduce the inhomogeneity of gas concentration distribution. Previous models [12], [15] have treated common dead space mixing and pendelluft as a single process and were unable to distinguish the relative effects of each. However, our model shows that the distribution of initial dead space gas to alveolar regions can have substantial effects, depending upon the end-expiratory volume and breathing rate, while the effects of pendelluft are less significant.

Typically, in experimental studies we deal with a specific mechanical system (i.e., one with a particular set of mechanical parameter values). In order to investigate pulmonary mechanical behavior and its effects on gas concentration distribution, we can alter the forcing function to produce changes in breathing frequency and volume operating point. From Figs. 5 and 6 and Table IV we see that these changes can substantially affect the distribution of the effective linearized mechanical properties as well as the mechanical variables (i.e., $V_i(E)$, V_{Ti}, λ_i, and V_p/V_T). Equation (A1) suggests that the effect of one of the links between mechanics and gas concentration distribution, namely, the distribution of the initial dead space gas (λ_i) to the compartments, can be reduced if larger tidal volumes are employed. This was not tested here because large values of V_T would increase static hysteresis, which is assumed negligible in this model.

Clinical Significance

For analyzing experimental (clinical) data, observable indexes are required (e.g., dynamic compliance C_d and moment ratio μ_1/μ_0 of the washout curve). As seen in Fig. 7, small changes in $V_L(E)$, even in the uniform lung, can greatly affect C_d at a given frequency; hence, graphs of C_d versus frequency obtained when $V_L(E)$ is not held constant can lead to erroneous conclusions. When used to characterize the washout curve, the moment ratio has high discrimination among clinical groups compared to other indexes [7]. As seen in Fig. 9, μ_1/μ_0 is always larger for the nonuniform obstructive lung than for the uniform normal lung. However, larger values of μ_1/μ_0 for the obstructed lung do not directly correspond to larger values of $\overline{\Delta X}$ (Table V). This is most likely due to the information lost in the calculation of μ_1/μ_0 when the washout curve is truncated, i.e., data for $\eta_k > 8$ are ignored.

Theoretically, the slope of the alveolar plateau should provide an observable index of intrapulmonary gas concentration distribution. In the example shown (Fig. 4), the alveolar plateau has a noticeable positive slope. Whether this behavior occurs and can be measured with sufficient accuracy for use as a quantitative index remains to be determined. We can, however, infer inhomogeneous intrapulmonary gas concentration distribution from a nonlinear, semilog washout curve. For the nonuniform mechanical system, the distribution of mechanical variables caused the washout curves (Fig. 8) to be dependent upon frequency and volume operating point.

Several investigators have attempted to relate inhomogeneous gas concentration distribution and pulmonary mechanics using linearized model concepts. For subjects with normal and diseased lungs, Chiang [2] had little success in correlating a mechanical time constant to a single exponential washout time constant. In another study, Chiang [3] found that dynamic compliance decreased with frequency in all subjects with nonlinear, semilog washout curves. However, as pointed out by Wanner *et al.* [18], a multibreath washout at only one frequency (as done by Chiang) is insufficient for relating gas concentration distribution and mechanical behavior. Indeed, our analysis suggests that performing washouts at more than one volume operating point may also be necessary.

Bouhuys *et al.* [1] found that the multibreath washout was independent of breathing frequency in normal subjects and symptom-free asthmatics. Washouts of subjects having chronic obstructive pulmonary disease, however, were shown to be frequency dependent [5]. Furthermore, Ingram and Schilder [10] found a frequency dependent washout only in subjects who showed a decrease in dynamic compliance greater than 20 percent. Based on our simulations, inferences about gas concentration distribution from the dynamic compliance data may not be valid unless end-expiratory lung volume and tidal volumes are invariant with frequency. That this may be a problem is suggested by studies of normal subjects that show a significant variability in the frequency dependence of dynamic compliance [9].

SUMMARY

Spatially lumped compartmental models of pulmonary mechanics and gas distribution are not meant to be isomorphic with lung anatomy. Indeed, in light of the complexity of this anatomy, the limited number of measurable, noninvasive variables, and the practical limitations on experimental procedures, development of isomorphic models for use in interpreting clinical data would be inappropriate. Instead, based on information about the behavior of the system and its various components, one may choose to conceptually lump (or combine) several of these components into representative (separate) functional units. With only two alveolar compartments and a common dead space, our model has the simplest form which permits a realistically detailed description of how mechanics affect gas concentration distribution during tidal breathing at various frequencies and volume operating points.

Of major importance is the model's ability to provide a clear understanding of how the mechanical parameters and pressure forcing function produce pendelluft, the distribution of initial dead space gas volume to the compartments, and the distribution of compartmental resting and tidal volumes. It also shows how these, in turn, affect interregional gas concentration distribution. A single model which can convey this information has not been available in the past. To study these phenomena clinically, transpulmonary pressure together with flow and end-tidal concentration of N_2 at the airway opening must be measured. For confidence in the inferences based on these measurements, our simulations indicate that experiments would have to be repeated at several breathing rates and volume operating points.

APPENDIX

A CONDITION FOR HOMOGENEOUS GAS CONCENTRATION DISTRIBUTION WITH SYNCHRONOUS FLOW

Consider alveolar compartments with synchronous flow in the same direction. Assume that at the end of expiration (indicated by E), the concentration of N_2 is equal to a constant $C(0)$ everywhere in the lung:

$$C_i(E) = C_D(E) = C(0) \qquad (i = 1, 2, \cdots, n).$$

(The perfectly mixed alveolar compartments are indicated by the subscript i and the unmixed dead space by D.) Now, the N_2 in the lung is diluted by a single inhalation of pure O_2. From the beginning of inhalation until the dead space is cleared ($t = t_D$), the volume of compartment i increases to

$$V_i(t_D) = V_i(E) + \lambda_i V_D \Rightarrow \lambda_i = [V_i(t_D) - V_i(E)]/V_D$$

where λ_i is the fraction of gas volume in the dead space volume (V_D) at $t = 0$ that is distributed to compartment i. During this clearance period, the N_2 concentration in compartment i is unchanged:

$$C_i(t_D) = C(0)$$

After the dead space is cleared, the N_2 concentration in compartment i is diminished by the inhaled O_2. Since the mass of N_2 in compartment i is unchanged during inhalation for $t > t_D$, we can write the static N_2 balance:

$$C(0)[V_i(E) + \lambda_i V_D] = C_i(1)[V_i(E) + V_{Ti}]$$

where $C_i(1)$ is the N_2 concentration at the end of this first inhalation and V_{Ti} is the tidal volume of compartment i. Hence,

$$X_i(1) = \frac{C_i(1)}{C(0)} = \frac{V_i(E) + \lambda_i V_D}{V_i(E) + V_{Ti}} \equiv [GDI(i)], \tag{A1}$$

where $X_i(1)$ is the normalized concentration of compartment i and $GDI(i)$ is the generalized dilution index of compartment i. During exhalation, $X_i(1)$ is unchanged. If all compartments have the identical N_2 concentrations at the end of inhalation, then for any two compartments i and j,

$$X_i(1) = X_j(1) \Rightarrow GDI(i) = GDI(j). \tag{A2}$$

If gas concentration distribution is inhomogeneous,

$$\Delta GDI = |GDI(i) - GDI(j)| = \Delta X(1) = |X_i(1) - X_j(1)|. \tag{A3}$$

This generalized condition for homogeneous gas concentration distribution assumes that the flows to the compartments are synchronous and in the same direction. Equation (A1) is similar to the condition derived by Wise and Defares [19]. If the gas volume which is present in the dead space at $t = E$ is distributed in the same proportion as the end-inspiratory volumes of all compartments, i.e.,

$$\lambda_i/\lambda_j = [V_i(E) + V_{Ti}]/[V_j(E) + V_{Tj}], \tag{A4}$$

then (A2) reduces to

$$\frac{V_i(E)}{V_i(0) + V_{Ti}} = \frac{V_j(E)}{V_j(0) + V_{Tj}} \tag{A5}$$

We define the simple dilution index (SDI) as

$$SDI(i) = \frac{V_i(E)}{V_i(E) + V_{Tj}}.$$

If (A4) holds, but gas concentration distribution is inhomogeneous

$$\Delta SDI = |SDI(i) - SDI(j)| = \Delta GDI = \Delta X(1). \tag{A6}$$

As the condition for homogeneity of gas distribution, many investigators have used

$$V_{Ti}/V_i(E) = V_{Tj}/V_j(E) \tag{A7}$$

which was proposed by Defares and Donleben [6]. This is derived by rearranging (A5). Consequently, (A6) is misleading since it guarantees homogeneity only when the special conditions of (A4) are true.

REFERENCES

[1] A. Bouhuys, S. Lichtnechert, C. Lundgren, and G. Lundin, "Voluntary changes in breathing pattern and N_2 clearance from lungs," *J. Appl. Physiol.*, vol. 16, pp. 1039–1042, 1961.

[2] S. T. Chiang, "Relationship between the time constants of *RC* networks and nitrogen washout in respiratory systems," *Aerosp. Med.*, vol. 42, pp. 1270–1274, 1971.
[3] —, "Distribution of ventilation and frequency-dependence of dynamic lung compliance," *Thorax*, vol. 26, pp. 721–726, 1971.
[4] J. H. Comroe, Jr., *et al.*, *The Lung*, 2nd ed. Chicago, IL: Year Book Medical, 1962.
[5] A. Cutillo, E. Omboni, and S. Delgrossi, "Effects of respiratory frequency on distribution of inspired gas in normal subjects and patients with chronic obstructive lung disease," *Amer. Rev. Resp. Dis.*, vol. 105, pp. 756–767, 1972.
[6] J. G. Defares and P. G. Donleben, "Relationship between frequency-dependent compliance and unequal ventilation," *J. Appl. Physiol.*, vol. 15, pp. 166–169, 1960.
[7] G. M. Fleming, E. H. Chester, J. Saniie, and G. M. Saidel, "Ventilation inhomogeneity using multibreath nitrogen washout: comparison of moment ratio and other indices," *Amer. Rev. Resp. Dis.*, vol. 121, pp. 789–796, 1980.
[8] W. S. Fowler, E. R. Cornish, Jr., and S. S. Kety, "Lung function studies. VIII. Analysis of alveolar ventilation by pulmonary nitrogen clearance curves," *J. Clin. Invest.*, vol. 31, pp. 40–50, 1952.
[9] A. R. Guyatt, J. A. Siddorn, H. M. Brash, and D. C. Fenley, "Reproducibility of dynamic compliance and flow-volume curves in normal man," *J. Appl. Physiol.*, vol. 39, pp. 341–348, 1975.
[10] R. H. Ingram and D. P. Schilder, "Association of a decrease in dynamic compliance with a change in gas distribution," *J. Appl. Physiol.*, vol. 23, pp. 911–916, 1967.
[11] P. T. Macklem and J. Mead, "Resistance of central and peripheral airways measured by retrograde catheter," *J. Appl. Physiol.*, vol. 22, pp. 395–401, 1967.
[12] R. E. Nye, Jr., "Theoretical limits to measurements of uneven ventilation," *J. Appl. Physiol.*, vol. 16, pp. 1115–1124, 1961.
[13] A. B. Otis, C. B. McKerrow, R. A. Bartlett, J. Mead, M. B. McElroy, N. J. Selverstone, and E. P. Radford, "Mechanical factors in distribution of pulmonary ventilation," *J. Appl. Physiol.*, vol. 8, pp. 427–443, 1956.
[14] T. J. Pedley, M. F. Sudlow, and J. Milic-Emili, "A nonlinear theory of the distribution of pulmonary ventilation," *Respir. Physiol.*, vol. 15, pp. 1–38, 1972.
[15] I. Safonoff and G. E. Emmanuel, "The effect of pendelluft and dead space on nitrogen clearance: mathematical and experimental models and their application to the study of the distribution of ventilation," *J. Clin. Invest.*, vol. 46, pp. 1683–1693, 1967.
[16] J. Saniie, G. M. Saidel, and E. H. Chester, "Real-time moment analysis of pulmonary nitrogen washout," *J. Appl. Physiol.*, vol. 46, pp. 1184–1190, 1979.
[17] D. L. Vawter, Y. C. Fung, and J. B. West, "Constitutive equation of lung tissue elasticity," *J. Biomech. Eng.*, vol. 101, pp. 38–45, 1979.
[18] A. Wanner, S. Zarzecki, N. Atkins, A. Zapata, and M. A. Sackner, "Relationship between frequency dependence of lung compliance and distribution of ventilation," *J. Clin. Invest.*, vol. 54, pp. 1200–1213, 1974.
[19] N. E. Wise and J. G. Defares, "A model for unequal ventilation of the lungs assuming a common dead space and two separate dead spaces," *Bull. Math. Biophys.*, vol. 21, 1959.

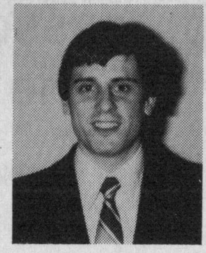

Kenneth R. Lutchen (S'80) received the B.S. degree in engineering science from the University of Virginia, Charlottesville, in 1977, and the M.S. degree in biomedical engineering from Case Western Reserve University, Cleveland, OH, in 1980.

He is now a Doctoral Candidate in Biomedical Engineering at Case Western Reserve University and has been a Graduate Research Assistant there since 1977. His current research is in the application of parameter estimation, sensitivity analysis, and experimental design techniques to nonlinear systems.

Mr. Lutchen is a member and former President of the Alpha Chapter of Tau Beta Pi.

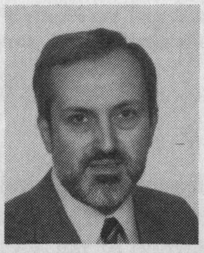

Frank P. Primiano, Jr. (S'67–M'70) received the B.S.M.E. degree in 1962 and the M.S.B.M.E. degree in 1963, both from Drexel University, Philadelphia, PA, and the Ph.D. degree in biomedical engineering in 1971 from Case Western Reserve University, Cleveland, OH.

He is currently Assistant Professor of Biomedical Engineering in Pediatrics at Case Western Reserve University and Research Director of the Pulmonary Function Laboratory, Rainbow Babies and Childrens Hospital, Cleveland, OH. His research interests include biomedical instrumentation and respiratory physiology, in particular, ventilatory mechanics and pulmonary function testing.

Dr. Primiano is a member of Sigma Xi, the Biomedical Engineering Society, the American Society of Mechanical Engineers, and the American Thoracic Society.

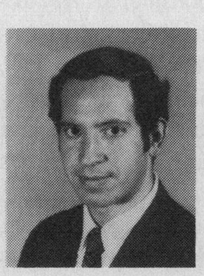

Gerald M. Saidel received the B.Ch.E. degree from Rensselaer Polytechnic Institute, Troy, NY, in 1960, and the Ph.D. degree in chemical engineering from Johns Hopkins University, Baltimore, MD, in 1965. After postdoctoral work as a National Science Foundation Fellow at the City College, New York, NY, he went to the Case Institute of Technology, Cleveland, OH, in 1966 as a Research Associate in Biomedical Engineering. Since 1967, he has been on the Faculty of Case Western Reserve University, Cleveland, OH, where he currently serves as Professor of Biomedical Engineering.

Dr. Saidel is Section Editor of the *Annals of Biomedical Engineering*.